Journal of Biological Physics **17**: 19–40, 1989.

Application of the Fröhlich Theory to the Modelling of Rouleau Formation in Human Erythrocytes

J. A. TUSZYŃSKI
Department of Physics, University of Alberta, Edmonton, Alberta, Canada T6G 2J1

and

E. KIMBERLY STRONG
St. John's College, Oxford University, Oxford 0X1 3JP, England

(Accepted: 25 August 1988)

Abstract. The details of Fröhlich's theory and some recent experiments on the rouleau formation of human erythrocytes which exhibit a strong interaction that appears to satisfy the prerequisites of the Fröhlich theory, are summarized. To verify whether the Fröhlich theory of long-range coherence in biological systems is applicable to the phenomenon of rouleau formation in human erythrocytes, the interactions between erythrocytes are modelled as those between two large, coupled oscillating dipoles. Relevant expressions for the resonant long-range and the van der Waals interaction are then derived. Using the available numerical data, the eigenfrequencies and the interaction energies corresponding to the experimental conditions are then derived. In the range of postulated frequencies (10^{11}–10^{12} Hz) the effective interaction coefficient Ξ due to the resonant long-range forces is, indeed, found to agree with its experimental value of 3.0. However, the same value of Ξ can also be achieved through the ordinary van der Waals interactions between dipoles oscillating at lower frequencies. It is concluded that the resonant long-range interaction between erythrocytes may be responsible for the onset of rouleau formation. However, other mechanisms cannot be ruled out at this stage, especially since the Fröhlich mechanism requires a number of unconfirmed preconditions.

Key words. Erythrocytes, rouleau formation, Fröhlich theory, dipole-dipole interactions, van der Waals forces.

1. Introduction

Due to constant supply of metabolic energy, many biological systems are considered to be far from thermodynamic equilibrium and in regions of nonlinear response to external forces. These systems also exhibit a high degree of order (understood in terms of functional organization rather than spatial arrangement), which suggests the presence of forces between the subsystems that are stronger than short-range chemical forces and screened Coulomb forces. Fröhlich (1978, 1980) suggested in his theory that if the components of a biological system undergo coherent elastic vibrations, then long-range interactions of either a repulsive or attractive nature can be strongly excited. This theory can be applied only to systems

which satisfy the following prerequisites:

(i) The existence of a high degree of organization which requires collective properties at the microscopic level.
(ii) The existence of a sufficiently strong cell membrane potential difference which will electrically polarize molecules within the membrane. A potential difference of about 10–100 mV is known to exist across biological membranes with thickness of 4–10 nm (Chance *et al.*, 1980). This results in an electric field of $1–25 \times 10^6$ V/m very strongly polarizing the membrane and possibly inducing an electret state.
(iii) The rate of supply of metabolic energy S must exceed a critical value S_0.

High-frequency longitudinal dipolar oscillations of sections of biological membranes can occur with displacements perpendicular to the surface (Fröhlich, 1980), so that the longest wavelength is twice the membrane thickness. The displacement involved characterizes the magnitude of the oscillating dipole moment as, for example, in the lipid head group. Using the speed of sound as 10^3 m/s as the propagation velocity of these membrane waves, their frequency is found as $\nu = 0.5–1.3 \times 10^{11}$ Hz or $\omega = 2\pi\nu = 3–8 \times 10^{11}$ Hz. There are several other mechanisms (Fröhlich, 1978) which can produce oscillations in this frequency range. For example, vibrations may take place through the interaction of successive ionic double layers or within large polar molecules such as DNA, RNA, proteins and hydrogen-bonded amides. Finally, the collective motion of ions freed in chemical reactions may lead to plasmon-type excitations. These oscillating cellular systems may interact amongst themselves, giving rise to narrow bands of coherent modes.

Various experiments were described by Fröhlich (1980) that demonstrate the sensitivity of metabolic processes to certain frequencies of electromagnetic radiation (especially in the microwave region). In some cases, such life processes as synthesis and reproduction exhibit resonant behavior at certain frequencies, while in others, there is a frequency-dependent absorption of radiation. Various spectroscopic experiments on living cells have also been performed with the objective of finding some nonthermal excitations of narrow frequency bands (Webb, 1980). Fröhlich (1980) concluded that these experiments cause biological effects that cannot be explained as simply due to heating or the direct-action of an applied electric field. Fröhlich (1980) made attempts to explain the observed nonthermal, nonlinear effects dependent on frequency, intensity, and time of irradiation, in terms of the theory of long-range coherence. However, the Fröhlich theory has not been conclusively confirmed experimentally yet.

To date, the most promising evidence in support of Fröhlich's conjecture comes from a series of experiments on the rouleau formation of human red blood cells (erythrocytes). Erythrocytes aggregate face-to-face in columns when blood ceases to flow and there are no shearing forces. This phenomenon exists only in mammals with flattened erythrocytes. We can only speculate at this point that the flattening is a result of a force acting within an erythrocyte and possibly leads to much stronger

inter-erythrocyte interactions which can now be axial. Clinically, the appearance of large rouleaux is an indicator of elevated blood plasma concentrations of certain macromolecules (Reich, 1978). Such neutral polymers as dextran, ficoll and polyvinyl pyrrolidone (PVP) enhance the rate of rouleau formation of erythrocytes suspended in saline solutions and blood plasmas, provided their molecular weight exceeds a threshold value. It is, therefore, natural to expect that these macromolecules are instrumental in transmitting or facilitating the attractive interactions between erythrocytes. The objective of this paper is to investigate whether or not the Fröhlich model is capable of providing an explanation of rouleau formation. Qualitative arguments for the Fröhlich theory were put forward in several recent papers of Rowlands *et al.* (1981, 1982, 1983). However, no quantitative analysis of the problem exists in the literature.

2. Experiments on Rouleau Formation

Human erythrocytes, when metabolically active, have a biconcave disc shape and are covered by a membrane of proteins embedded in a lipid bilayer (see Figure 1). The mass of an erythrocyte is of the order of 10^{-15} kg, its density 1.15×10^3 kg/m^3 and surface area 140 μm^2 (Steck, 1974). Most of the cell's membrane is composed of proteins (52%) and lipids (40%), with a remaining 8% of carbohydrates. When erythrocytes collide during a seemingly random motion, they slide face-to-face and adhere together to form long, cylindrical and sometimes branched structures called rouleaux (see Figure 2).

The first set of experiments of Rowlands *et al.* (1981) involved time lapse photography. Pairs of cells that were initially less than one diameter (8 μm) apart were observed until they collided. Assuming random motion, the theoretical average probability of such pairs colliding was calculated as approximately 0.3. In contrast, under normal conditions, the observed fraction of pairs colliding was 0.85 ± 0.06 suggesting the existence of a strong attractive interaction between

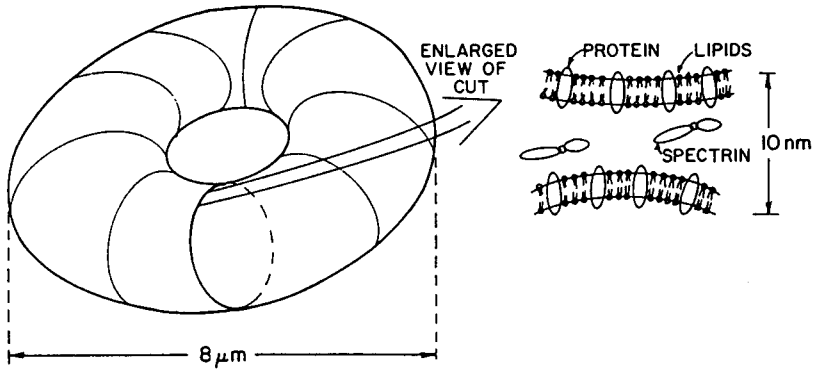

Fig. 1. A typical erythrocyte.

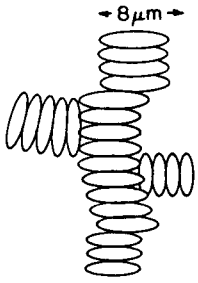

Fig. 2. A typical rouleau.

erythrocytes. When the pH was reduced from 7.6 to 6.3 (drastically reducing the membrane's potential difference since its net isoelectric point lies in the range of 4–5 pH), the fraction of collisions decreased to 0.33. Restoring the pH to 7.6 resulted in the fraction becoming 0.76. Introducing ionophores to depolarize the cell membrane reduced the fraction to 0.48. Metabolically depleting the erythrocytes by washing them and then incubating them in phosphate-buffered saline (PBS), reduced the fraction to 0.39, and repleting them by incubation in adenosine restored the fraction to 0.75. Finally, fixing the erythrocytes with gluteraldehyde which cross links proteins and destroys cellular organization also decreased pair collisions to the random value. The second set of experiments of Rowlands *et al.* (1982) resulted in the determination of an interaction coefficient based upon Smoluchowski's theory of colloidal coagulation. The equation governing the kinetics of coagulation (with the effect of cell sedimentation reducing the process from three to two spatial dimensions) is

$$\frac{1}{N_t} - \frac{1}{N_0} = \frac{2k_B T}{3\eta} \left(\frac{r_0^*}{r_0}\right) t, \tag{1}$$

where N_t is the total number of particles (single and aggregate) at time t, N_0 is the initial number of particles, k_B ($= 1.38 \times 10^{-23}$ J/k) is Boltzmann's constant, T is the absolute temperature, η is the viscosity, r_0 is the average radius of the particles and r_0^* is a parameter defining the radius of a zone of attraction around each cell. This equation is based upon the Stokes–Einstein definition of the diffusion coefficient for spheres $D = k_B T/6\pi\eta r_0$. The interaction coefficient $\Xi = r_0^*/r_0$ indicates how many times faster the actual aggregation process is taking place than for Brownian motion and its experimental values are shown in the left-hand part of Table I. It was concluded by Rowlands *et al.* (1981) that the attractive interaction disappears when the three requirements of the Fröhlich theory are no longer met.

Fritz (1984) performed quasi-elastic light scattering experiments from solutions with suspensions of erythrocytes using a photomultiplier to detect the scattered laser light. The solution used in these experiments was PBS at various pH, to which human serum albumin (HSA) was added. The additional macromolecules were PVP at several molecular weights. The PVP at the molecular weight of 360 000 caused an abnormally high diffusion coefficient under the conditions of metabolic activity and with the presence of a transmembrane field. Once again, the influence

Table I. The interaction coefficient Ξ_R as measured by Rowlands *et al.* (1982) and the corresponding values of the diffusion coefficient D and the interaction coefficient Ξ_F as measured by Fritz (1984), under various conditions

Conditions	Probability	Ξ_R	D(in 10^{-10} cm^2/s)	Ξ_F
Normal cells	0.85	2.92 ± 1.12	23.5	3.07
Cells at pH 6.3	0.40	1.07 ± 0.41	19.5	1.89
Cells restored to pH 7.6	0.71	2.57 ± 0.99	21.5	2.49
Ionophore-treated cells	0.48	1.69 ± 0.04	–	–
Metabolically depleted cells	0.44	0.43 ± 0.11	17.5	1.26
Cells repleted with adenosine	0.87	3.26 ± 0.68	22.2	2.70
Gluteraldehyde fixed cells	0.46	0.92 ± 0.46	15.1	0.53
Microspheres 3.4 μm	0.24	0.72 ± 0.00	15.0	0.50
Microspheres 5.9 μm	–	0.92 ± 0.00	–	–
Microspheres 8.0 μm	–	1.15 ± 0.00	–	–

of macromolecules on the rate of rouleau formation is quite dramatic, indicating their possible role in transmitting the interaction. Several conditions of metabolic activity and the pH were tested in order to independently verify earlier findings of Rowlands *et al.* (1982). In order to make a quantitative comparison between the two sets of experiments, the difference in dimensionality and the particle concentrations used in both experiments must be accounted for: $\rho_R = 5 \times 10^{-3}$ v/v in the first and $\rho_F = 1.8 \times 10^{-4}$ v/v in the second. Using the first order approximation in the virial expansion, the interaction coefficient Ξ_F corresponding to Fritz's experiment can be calculated from his diffusion constant D as (Paul *et al.*, 1983):

$$\Xi_F = \frac{1}{2}\left[1 + \left(\frac{\rho_R}{\rho_F}\right)^{2/3}\left(\frac{D}{D_0} - 1\right)\right], \tag{2}$$

where D_0 is the diffusion coefficient under Brownian motion with no forces present. The values of Ξ_F are shown in Table I. It is clear that both types of experiments yield remarkably close results for Ξ.

Finally, Blinowska *et al.* (1985) performed an experiment in order to find the suspected resonant frequency in the microwave absorption spectra. The absorption spectra were measured for both normal erythrocytes and the ghosts, with highly concentrated, thin samples, and a low-frequency range chosen, in order to reduce the absorption effects of the buffer solution. A resonance peak indeed appeared at 0.367×10^{11} Hz for both the erythrocytes and the ghosts, and was stronger for the latter.

3. The Theoretical Model

The starting point in our analysis is to follow Fröhlich (1980) and assume that within each cell membrane there is a large number of oscillating dipolar segments which are coupled together via a combination of elastic and electric forces. The main conjecture is that a metabolically active cell, e.g. a red blood cell, exhibits

Bose condensation and from among a very large number of possible oscillation frequencies the cell selects a characteristic frequency (or a narrow band). The question of how and why this type of effect should arise is a separate problem which has been addressed in the past by many researchers in the field and shall not be pursued here. Having accepted the Fröhlich conjecture on a trial basis we then model erythrocytes as large dipoles oscillating with certain initial frequencies. Their mutual interactions are of dipole-dipole type and, hence, the effective Hamiltonian for a pair of interacting erythrocytes (neglecting many other degrees of freedom) is that of two coupled harmonic oscillators (Fröhlich 1972)

$$H = \frac{1}{2}\sum_{i=1}^{2} M_i(\dot{u}_i^2 + \omega_i^2 u_i^2) - \frac{1}{2}\sum_{i\neq j=1} u_i T_{ij} u_j \tag{3}$$

which leads to the (coupled) equations of motion for the displacements u_i

$$M_i(\ddot{u}_i + \omega_i^2 u_i) = u_j T_{ji} \quad (\mathrm{i} = 1, 2), \tag{4}$$

where M_i is the mass of the ith dipole and the interaction potential is

$$T_{ij} = \gamma^2 e^2 (Z_i Z_j)^{1/2} / r_{ij}^3 \varepsilon_0 \varepsilon'(\omega). \tag{5}$$

The following notation has been adopted above: $\gamma^2 = (\cos\gamma_0 - \cos^3\gamma_0)$ and γ depends on the geometry of the system as shown in Figure 3 following Pokorny (1980). In Figure 3, S_1 is the circular effective interaction layer for the cells which consists of elementary oscillating electric dipoles with their axes perpendicular to S_1. Since the cells slide face to face, only the most favorable orientation has been included, i.e. when their dipole moments are parallel. In Equation (5), e ($= 1.6 \times 10^{-19}$ C) is the elementary charge, Z_i is the number of elastically bound particles within the ith dipole, r_{ij} is the distance between dipoles i and j (greater than dipole diameter L) or more precisely the distance between the effective interaction layers, ε_0 ($= 8.85 \times 10^{-12}$ $\mathrm{C^2 N^{-1} m^{-2}}$) is the permittivity of vacuum and $\varepsilon'(\omega)$ is the real part of the frequency-dependent dielectric constant of the medium. Seeking the solutions of Equation (4) as normal modes $u_i = u_i^0(\omega)\, \mathrm{e}^{-i\omega t}$ and substituting it into Equation (4) gives the eigenfrequencies fo the interacting system as

$$\omega_{\pm} = \left\{\frac{1}{2}(\omega_1^2 + \omega_2^2) \pm \left[\frac{1}{4}(\omega_1^2 - \omega_2^2)^2 + \frac{T_{12}\, T_{21}}{M_1\, M_2}\right]^{1/2}\right\}^{1/2}. \tag{6}$$

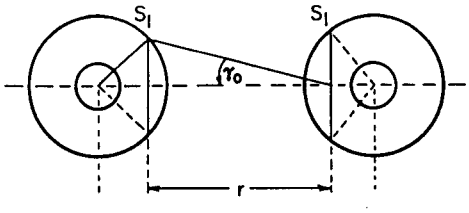

Fig. 3. Geometrical illustration of two interacting erythrocytes where S_1 is the effective interaction layer and r is the distance between S_1 and S_2, following Pokorny (1980).

This expression simplifies somewhat for the case of two identical dipoles where $M_1 = M_2 = M$; $T_{12} = T_{21} = T$, $Z_1 = Z_2 = Z$ and $r_{12} = r$, so that

$$\omega_{\pm}^2 = \frac{1}{2}(\omega_1^2 + \omega_2^2) \pm \left[\frac{1}{4}(\omega_1^2 - \omega_2^2)^2 + \frac{T^2}{M^2}\right]^{1/2}. \tag{7}$$

This becomes particularly interesting at resonance, when $\omega_1 = \omega_2 = \omega$, and the eigenfrequencies for the two identical dipoles are

$$\omega_{\pm} = \left(\omega^2 \pm \frac{T}{M}\right)^{1/2}. \tag{8}$$

The condition of resonance for two only approximately equal cells is, of course, an idealization. It is assumed, however, that the external conditions which are very crucial in establishing a given ω are identical and that the interactions are relatively weak between the cells to allow the present treatment. A more appropriate treatment which is planned for future calculations should allow for an uncertainty in both ω and in the interaction constant. The ensuing calculation would search for the occurrence of resonance under these imperfect conditions.

Since the dielectric constant is strongly frequency-dependent, the interaction constant T in Equation (8) is an implicit function of $\omega_{\pm}$. Thus, denoting $\beta^2 = \gamma^2 e^2 Z / M r^3 \varepsilon_0$, gives

$$\omega_{\pm}^2 = \omega^2 \pm \frac{\beta^2}{\varepsilon'(\omega_{\pm})}. \tag{9}$$

The dielectric constant of a biological system can be approximated as (Grant *et al.*, 1978)

$$\varepsilon'(\omega) \cong v_m \varepsilon'_m(\omega) + v_b \varepsilon'_b(\omega) + (1 - v_m - v_b)\varepsilon'_w(\omega), \tag{10}$$

where v_m and v_b are the volume fractions of the membrane dipoles and the bound water, respectively, and ε'_m, ε'_b, and ε'_w are the real parts of the dielectric constants of the membrane dipoles, the bound water, and the free water, respectively. Bound water (or hydration water) is composed of H_2O molecules which are attached due to dipole-dipole forces to the many polar macromolecules such as proteins, DNA, RNA, etc. (Hasted, 1973). This type of water, as opposed to free water with random arrangement of its dipole moments, is often in an electret state possessing a net dipole moment. The contribution from bound water is quite small since $v_b \ll v_w$, and since bound water relaxes at frequencies below those of interest. The membrane dipoles have already been included in the dynamics analysis resulting from the Hamiltonian of Equation (3). Although they also may be suspected of giving rise to resonance peaks in the region of interest, there is little experimental data allowing appropriate calculations to be made at the present time. Therefore, as a simplification $\varepsilon'(\omega)$ is here approximated by that of free water, i.e. $\varepsilon'(\omega) = \varepsilon'_w(\omega)$. The latter is given by the Debye equation (Fröhlich 1958)

$$\varepsilon'(\omega) = \varepsilon_\infty + \frac{\varepsilon_s - \varepsilon_\infty}{1 + \omega^2 \tau^2}, \tag{11}$$

where ε_s is the static dielectric constant $\varepsilon_s = \varepsilon'(0)$, ε_∞ is the optical dielectric constant, $\varepsilon_\infty = \varepsilon'(\infty)$, and τ is the relaxation time. At room temperature the free water parameters are (Grant *et al.*, 1978): $\varepsilon_\infty = 4.5$, $\varepsilon_s = 78.5$ and $\tau = 0.9 \times 10^{-11}$ s. Now substituting $\omega = \omega_\pm$ into Equation (11) and then substituting Equation (11) into Equation (9) yields an equation for the resultant frequency which can now be split into up to four different values $\omega_{ij} (i = \pm 1$ and $j = \pm 1)$

$$\omega_{ij} = \{[C_i + \eta_j \sqrt{C_i^2 + 4\varepsilon_\infty \tau^2 (\varepsilon_s \omega^2 + \eta_i \beta^2)}]/2\varepsilon_\infty \tau^2\}^{1/2}, \tag{12}$$

where $C_i = \varepsilon_\infty \omega^2 \tau^2 - \varepsilon_s + \eta_i \beta^2 \tau^2$ and $\eta_i = \pm 1$, $\eta_j = \pm 1$. Using the data elaborated on in the next section, we have plotted the split frequencies in Figure 4. Note that the splitting first occurs at $\omega^* = 0.41 \times 10^{11}$ Hz and persists up to approximately

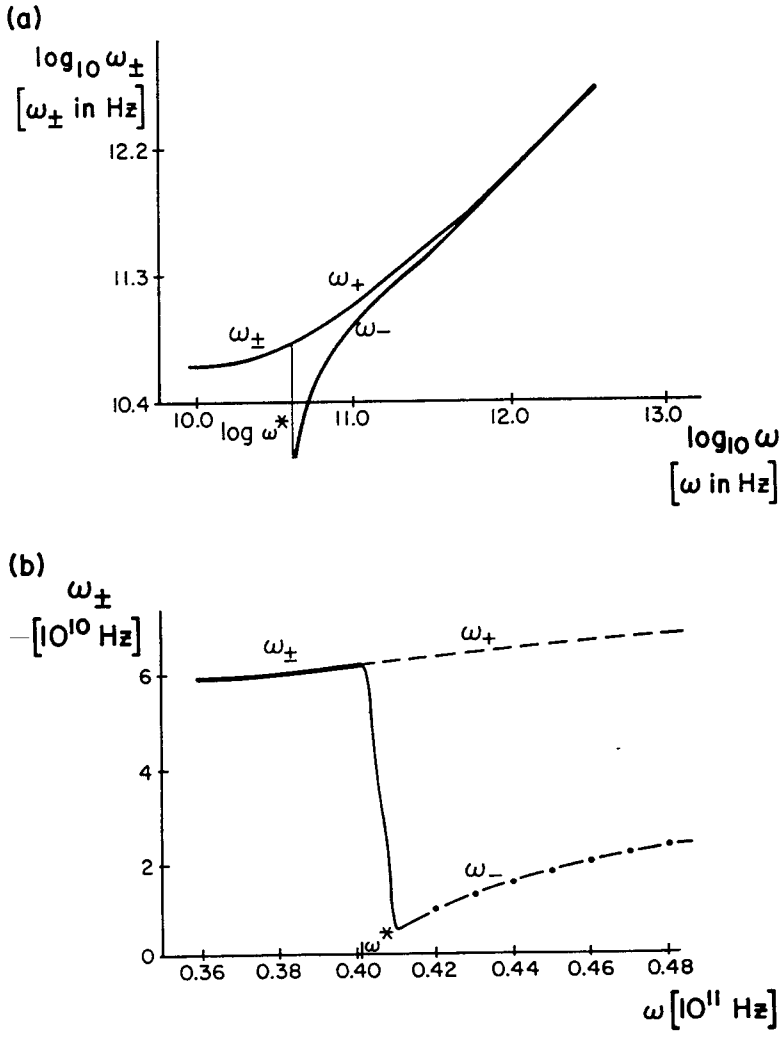

Fig. 4. (a) A graph of $\log_{10} \omega_\pm$ as a function of $\log_{10} \omega$ based on Equation (12) and the data presented in Section 4; (b) A close-up of the graph of $\omega_\pm$ as a function of ω in the vicinity of ω^*.

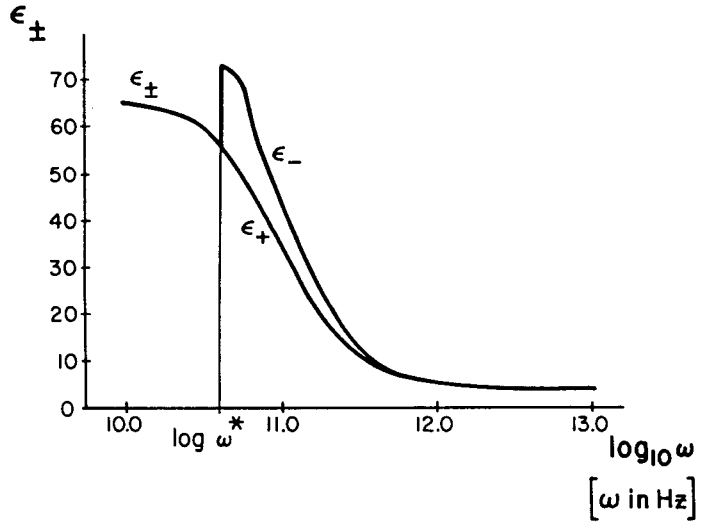

Fig. 5. A graph of ε'_+ and ε'_- as a function of $\log_{10}\omega$ based on Equation (13) and the data presented in Section 4.

10^{12} Hz. This, then is the range of frequencies within which the long-range interaction predicted by Fröhlich (1980) may exist. An explicit expression can also be obtained for $\varepsilon'_{ij}(\omega_{ij})$ as

$$\varepsilon'_{ij} = \varepsilon_\infty + (\varepsilon_s - \varepsilon_\infty)/[2\varepsilon_\infty + C_i + \eta_j\sqrt{C_i^2 + 4\varepsilon_\infty\tau^2(\varepsilon_s\omega^2 + \eta_j\beta^2)}]\,. \tag{13}$$

Using the data of the next section, we have plotted the behavior of ε' as a function of frequency in Figure 5.

Tuszyński (1985) recently demonstrated that long-range interactions may also occur at resonance in systems comprised of N interacting dipole moments (erythrocytes). Then, the interaction energy resulting from changing the distribution of oscillation frequencies from $\{\omega_i;\ i = 1, \ldots, N\}$ to $\{\Omega_i;\ i = 1, \ldots, N\}$ is given by

$$\Delta E = kT\sum_{i=1}^{N} \ln\left[\frac{\sinh(\hbar\Omega_i/2k_BT)}{\sinh(\hbar\omega_i/2k_BT)}\right]. \tag{14}$$

Such an approach is much more realistic in our applications to rouleau formation, since each erythrocyte can be viewed as a multi-mode rather than a single-mode oscillator. Therefore, assuming the total number of quasi-particles (longitudinal phonons) to be n in each erythrocyte and that the resultant occupation numbers of the extremal frequencies ($\omega_+ = \max\{\Omega_i;\ 1 \leqslant i \leqslant N\}$ and $\omega_- = \min\{\Omega_i;\ 1 \leqslant i \leqslant N\}$) are n_+ and n_-, respectively, Equation (14) becomes

$$\Delta E = 2nk_BT\left\{f_+ ln\left[\frac{sinh(\hbar\omega_+/2k_BT)}{sinh(\hbar\omega_1/2k_BT)}\right] + f_- ln\left[\frac{sinh(\hbar\omega_-/2k_BT)}{sinh(\hbar\omega_2/2k_BT)}\right]\right\}, \tag{15}$$

where $f_\pm = n_\pm/n$ represents the fraction of quasi-particles occupying the mode $\omega_\pm$. Note that in nonequilibrium situations, $f_\pm$ depends on the rate of pumping of energy into the mode $\omega_\pm$. In thermodynamic equilibrium, $f_\pm$ represents an average

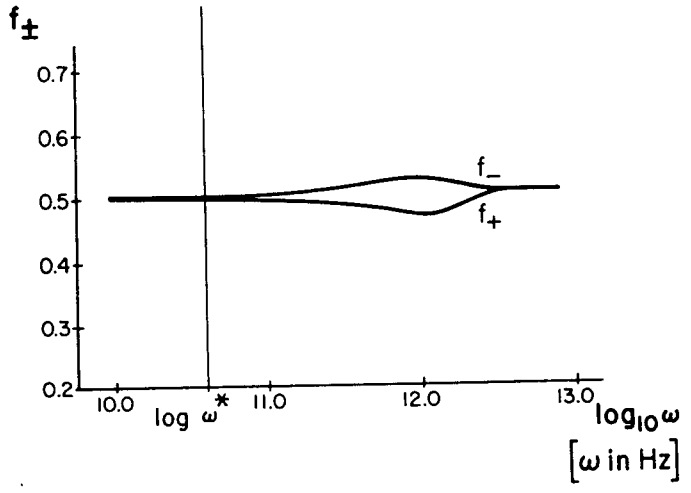

Fig. 6. A graph of f_+^{eq} and f_-^{eq} as a function of $\log_{10}\omega$ based on Equation (16) and the data presented in Section 4.

occupation number of the mode $\omega_\pm$ and is, in general, given by Bose–Einstein distribution

$$f_\pm^{eq} = [e^{\hbar(\omega_\pm - \mu)/k_B T} - 1]^{-1}, \tag{16}$$

where the chemical potential μ can be easily found as

$$\mu = -k_B T \ ln\{[e_+ + e_- + (e_+^2 + e_-^2 - e_+ e_-)^{1/2}]/e_+ e_-\}, \tag{17}$$

where $e_\pm = \exp(\hbar\omega_\pm / k_B T)$. The plot of $f_\pm^{eq}$ for the relevant data is given in Figure 6. In particular, if $\hbar\omega \ll k_B T$, then a classical approximation is obtained: $f_\pm^{eq} \cong k_B T/\hbar(\omega_\pm - \mu)$ with $\mu \cong 2k_B T/\hbar$. On the other hand, if $\hbar\omega \gg k_B T$, then a quantum approximation is obtained:

$$f_\pm^{eq} \cong \exp\left[-\frac{\hbar}{k_B T}(\omega_\pm - \mu)\right]$$

with

$$\mu \cong -\frac{kT}{\hbar} \ln\left[\exp\left(-\frac{\hbar\omega_+}{k_B T}\right) + \exp\left(-\frac{\hbar\omega_-}{k_B T}\right)\right].$$

Since, in general, such considerations must include nonequilibrium conditions, f_+ and f_- will be left as parameters yet to be specified. Assuming that the dipole coupling is sufficiently weak ($\omega^2 \gg \beta^2/\varepsilon'$), Equation (9) is expanded showing an explicit dependence on the separation between the dipoles.

$$\omega_\pm \cong \omega \pm \frac{\beta^2}{2\omega\varepsilon'_\pm} - \frac{\beta^4}{8\omega^3 \varepsilon'^2_\pm} + \cdots, \tag{18}$$

where $\varepsilon'_\pm = \varepsilon'(\omega_\pm)$. Using Equation (15) in the extreme quantum case, which at

room temperatures $T = 300$ K implies frequencies much greater than 10^{13} Hz, ΔE can be approximated by

$$\Delta E_q \cong n\hbar[f_+\omega_+ + f_-\omega_- - (\omega_1 + \omega_2)] \xrightarrow[\omega_1 \to \omega_2]{} -\frac{A_q}{r^3} - \frac{B_q}{r^6}, \tag{19}$$

where we have shown the transition to resonance with A_q being the long-range coefficient arising only under the special conditions of resonance between dipolar oscillations on the two erythrocytes

$$A_q \cong -\frac{n\hbar}{2\omega}\left(\frac{\gamma^2 e^2 Z}{\varepsilon_0 M}\right)\left(-\frac{f_+}{\varepsilon'_+} + \frac{f_-}{\varepsilon'_-}\right) \tag{20}$$

and B_q being the van der Waals coefficient arising for arbitrary values of frequencies

$$B_q \cong \frac{n\hbar}{8\omega^3}\left(\frac{\gamma^2 e^2 Z}{\varepsilon_0 M}\right)^2\left(\frac{f_+}{\varepsilon'^2_+} + \frac{f_-}{\varepsilon'^2_-}\right). \tag{21}$$

In the extreme classical case with weak coupling, which at room temperature implies frequencies much lower than 10^{13} Hz, the interaction energy is given by

$$\Delta E_c = 2nk_B T[f_+ \ln(\omega_+/\omega_1) + f_- \ln(\omega_-/\omega_2)] \xrightarrow[\omega_1 \to \omega_2]{} -\frac{A_c}{r^3}\frac{B_c}{r^6}, \tag{22}$$

where A_c is the long-range coefficient

$$A_c \cong -\frac{nk_B T\gamma^2 e^2 Z}{\omega^2 \varepsilon_0 M}\left(-\frac{f_+}{\varepsilon'_+} + \frac{f_-}{\varepsilon'_-}\right) \tag{23}$$

and B_c is the van der Waals coefficient.

$$B_c \cong \frac{nk_B T}{2\omega^4}\left(\frac{\gamma^2 e^2 Z}{\varepsilon_0 M}\right)^2\left(\frac{f_+}{\varepsilon'^2_+} + \frac{f_-}{\varepsilon'^2_-}\right). \tag{24}$$

Typical plots of A_c and B_c as functions of ω are shown in Figures 7a and 7b, respectively. For the general case, in between these two extremes, the interaction energy Equation (15) can be expanded and dropping the terms of orders higher than β^4 its coefficients are found as follows: the long-range coefficient

$$A_i = A_q \coth x \tag{25}$$

and the van der Waals coefficient

$$B_i = B_q[\coth x - x(1 - \coth x)], \tag{26}$$

where $x = \hbar\omega/2k_B T$. Note that these expressions are valid in both regimes since when $x \ll 1$, then $\coth x = x^{-1}$ and

$$A_i \xrightarrow[x \to 0]{} A_q\left(\frac{1}{x}\right) = A_c \quad \text{and} \quad B_i \xrightarrow[x \to 0]{} B_q\left(\frac{2}{x}\right) = B_c.$$

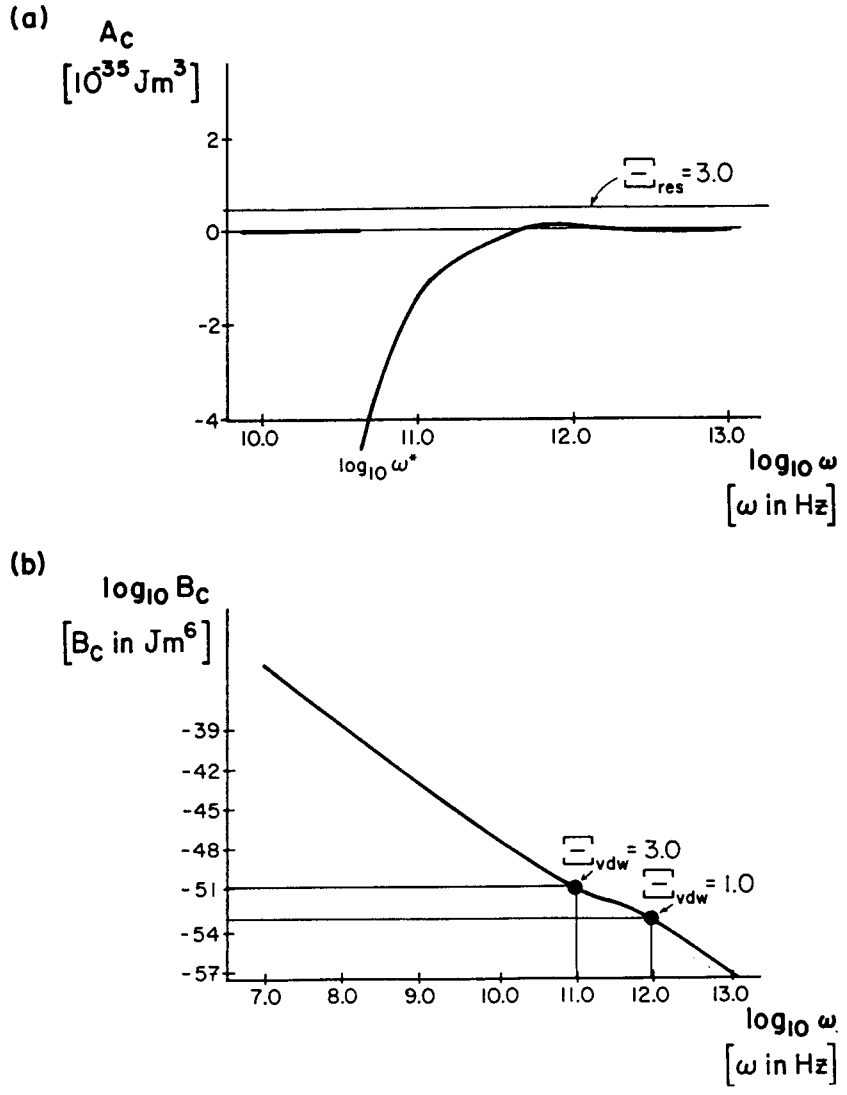

Fig. 7. A graph of (a) A_c of Equation (23) and (b) $\log_{10} B_c$ of Equation (24), as a function of $\log_{10}\omega$ plotted using the data presented in Section 4 and assuming thermal equilibrium conditions. Note that B_c is in units of Jm^6.

On the other hand, when $x \gg 1$, then $\coth x \to 1$ and

$$A_i \xrightarrow[x\to\infty]{} A_q \quad \text{and} \quad B_i \xrightarrow[x\to\infty]{} B_q .$$

The effect of temperature on the values of long-range coefficient A_i and the van der Waals coefficient B_i is shown in Figure 8.

It should be emphasized that the long-range contribution to ΔE proportional to A exists only under the conditions of resonance between the dipoles. In all other situations, i.e. when the two dipoles vibrate at arbitrary frequencies, the van der Waals contribution completely dominates ΔE with A being identically equal to zero. Hence, long-range interactions are very specific. Although in the present calculations we have assumed that $\omega_1 = \omega_2$ when calculating both the long-range and

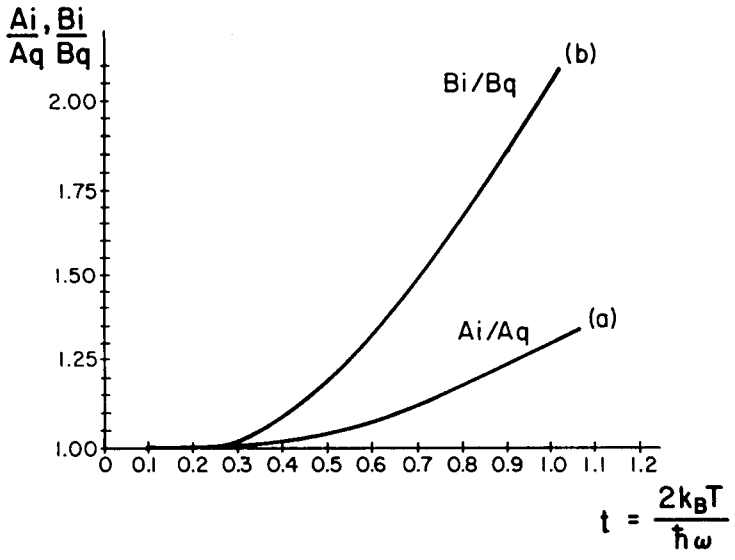

Fig. 8. A graph of (a) A_i/A_q and (b) B_i/B_q as a function of $t = 2k_BT/\hbar\omega$.

the van der Waals contributions, that assumption is not needed in the latter case. Even if $\omega_1 \neq \omega_2$ the van der Waals term exists and the inclusion of the resonance condition was mainly provided for comparison purposes. Should we wish to make use of our resonance calculations in the general case, provided ω_1 and ω_2 do not differ too drastically, the value of ω in Equation (26) can be interpreted as an average frequency of the two dipole oscillations.

From Equation (26) it is obvious that the van der Waals interaction is always attractive, irrespective of the frequency range, temperature range or the type of the dielectric medium. However, as can be seen from Equation (25), the long-range interaction constant A_i may be repulsive ($A_i < 0$), attractive ($A_i > 0$) or zero depending on a delicate balance between $f_\pm$ and $\varepsilon'_\pm$. The form of A_i is too complicated to make general predictions for arbitrary values of ω and T, but a few special cases can be discussed. First of all, in thermodynamic equilibrium and for very high frequencies (but still within the classical limit), i.e. $\omega^2 \gg (\beta^2/\varepsilon_\infty - \varepsilon_s/\varepsilon_\infty \tau^2)$, the difference between ε_+ and ε_- practically disappears ($\varepsilon'_+ \cong \varepsilon'_-$). Since $f_+ < f_-$, we obtain $A_c < 0$ which means that the long-range contribution is repulsive. However, it is expected to be of negligible strength since $(f_+ - f_-)$ is normally extremely close to zero. Also in thermodynamic equilibrium, if the coupling constant β^2 is small, then the difference between ω_+ and ω_- is negligible resulting in $\varepsilon'_+ \cong \varepsilon'_-$ and $f_+ \cong f_-$. Since $\varepsilon_+ < \varepsilon_-$, for a vast majority of biological materials and arbitrary frequency ranges ($\varepsilon'(\omega)$ is almost always a monotonically decreasing function of frequency), we obtain $A_c > 0$ which means that the long-range contribution is very weak and attractive. Compared to thermodynamic equilibrium conditions, arbitrary population distributions via nonequilibrium pumping mechanisms, lead to much stronger interactions, since cancellation effects between the pairs of f_+ and f_- and ε_+ and ε_- may be eliminated. If, for example, the ω_- mode is pumped (i.e. $f_+ \to 0$

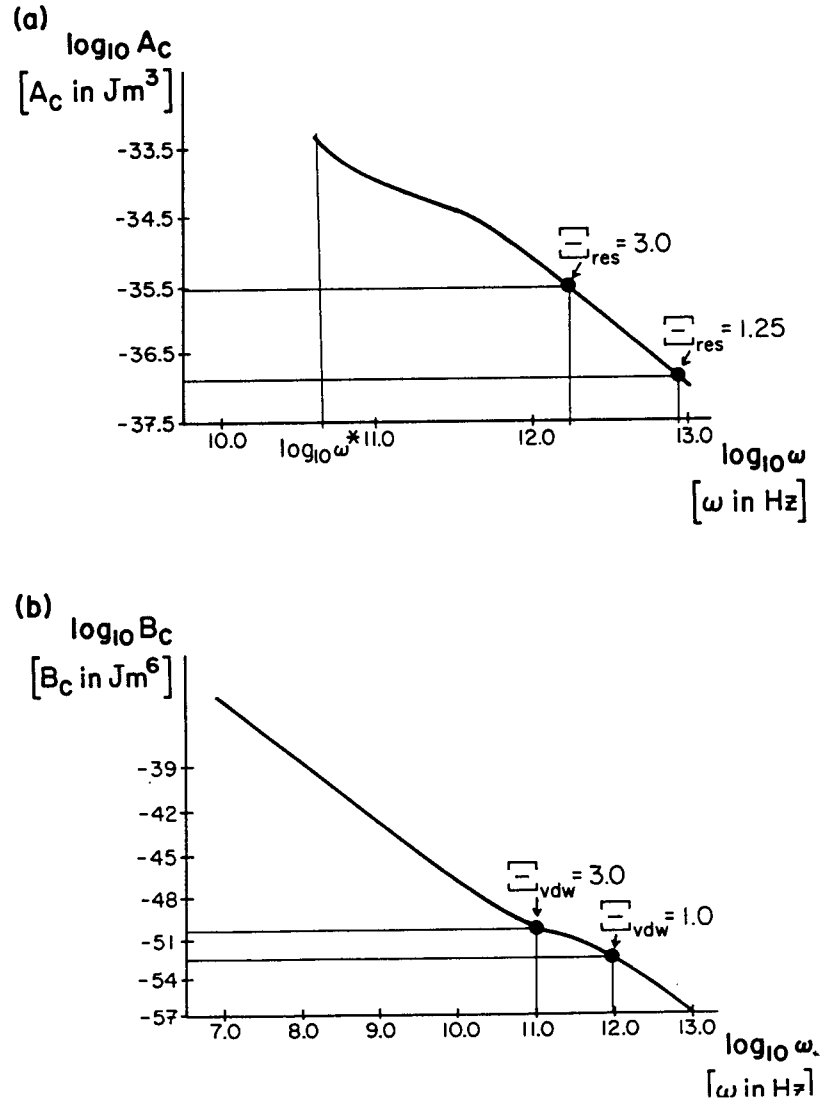

Fig. 9. A graph of (a) $\log_{10} A_c$ of Equation (23) and (b) $\log_{10} B_c$ of Equation (24), as a function of $\log_{10} \omega$ plotted using the data presented in Section 4 and assuming nonequilibrium conditions of occupation inversion (i.e. $f_+ = 1.0, f_- = 0.0$). Note that A_c is in units of Jm^3 and B_c in units of Jm^6.

while $f_- \to 1$), then a very strong repulsive long-range force arises in the system in agreement with Fröhlich's earlier predictions. On the other hand, if the ω_+-mode is pumped (population inversion, i.e. $f_- \to 0$ while $f_+ \to 1$), then a very strong attractive long-range force arises in the system. These nonequilibrium situations lead to A_c whose absolute value is greater by several orders of magnitude than that under equilibrium conditions. At the same time, the values B_c are essentially unchanged. This has been illustrated in Figure 9. Of course, in all cases the total potential vanishes as $r \to \infty$ and is attractive on short distances due to the stronger divergence of the van der Waals potential as $r \to 0$. In the case of repulsive long-range forces ($A_c < 0$), however, there will be a potential barrier whose maximum height is $A_c^2/4B_c$ which occurs at the distance $\bar{r} \equiv (2B_c/|A_c|)^{1/3}$. Thus, the stronger the

repulsion through A_c, the more difficult it is to overcome this barrier and the farther away it is felt by the interacting particles.

4. The Kinetics of Rouleau Formation

A general description of the kinetics of rouleau formation has recently been given by Paul *et al.* (1983) using the formalism of colloidal coagulation. The basic kinetic equation is

$$-\frac{dN}{dt} = 8\pi D r_0^* N^2, \tag{27}$$

where the symbols used have been explained below Equation (1). In order to describe the process, it is sufficient to parameterize it by the interaction coefficient $\Xi = r_0^*/r_0$, where r_0^* is defined through the inter-particle potential as

$$(r_0^*)^{-1} = \int_{r_0}^{\infty} dr\, r^{-2} \exp(\Delta E_i/k_B T). \tag{28}$$

It is useful to note that if the resonant long-range interaction is dominant, $(\Delta E_i \cong -A_i/r^3)$, then the interaction coefficient can be expressed using the incomplete gamma function and its power series expression (valid only for small values of the argument) as

$$\begin{aligned}\Xi_{res}^{-1} &= (r_0/3)(k_B T/A_i)^{1/3}\, \gamma\left(\frac{1}{3}, A_i/k_B T r_0^3\right) \\ &= (1/3) \sum_{n=0}^{\infty} \frac{(-1)^n}{n!(n+1/3)} \left(\frac{A_i}{k_B T r_0^3}\right)^n.\end{aligned} \tag{29}$$

On the other hand, if the van der Waals interaction is dominant ($\Delta E \cong -B_i/r^6$), then the interaction coefficient can be expressed as

$$\begin{aligned}\Xi_{vdw}^{-1} &= (r_0/6)(k_B T/B_i)^{1/6}\, \gamma\left(\frac{1}{6}, B_i/k_B T r_0^6\right) \\ &= (1/6) \sum_{n=0}^{\infty} \frac{(-1)^n}{n!(n+1/6)} \left(\frac{B_i}{k_B T r_0^6}\right)^n.\end{aligned} \tag{30}$$

We have written a short FORTRAN program to calculate both Ξ_{res} and Ξ_{vdw}. The results of these calculations are plotted in Figures 10a and 10b, respectively. Only the cases when both the long-range interaction and the van der Waals interaction are attractive ($A_i > 0$; $B_i > 0$) need be shown since in the case of repulsive potentials, it is well-known that Ξ does not exceed 1.0. Thus, it is clear from Figure 10a that in order for Ξ to exceed 3.0 (pertaining to the case of metabolic activity) $u \equiv r_0/(A_i/k_B T)^{1/3}$ must be less than 0.4. Using the known value of $r_0 = 4 \times 10^{-6}$ m, and $T = 293$ K, the lower limit on A_i in this situation is obtained as $A_i \geqslant 4 \times 10^{-36}$ Jm^3. On the other hand, for the long-range interaction to be negligible in the process of rouleau formation under the conditions of metabolic activity, it

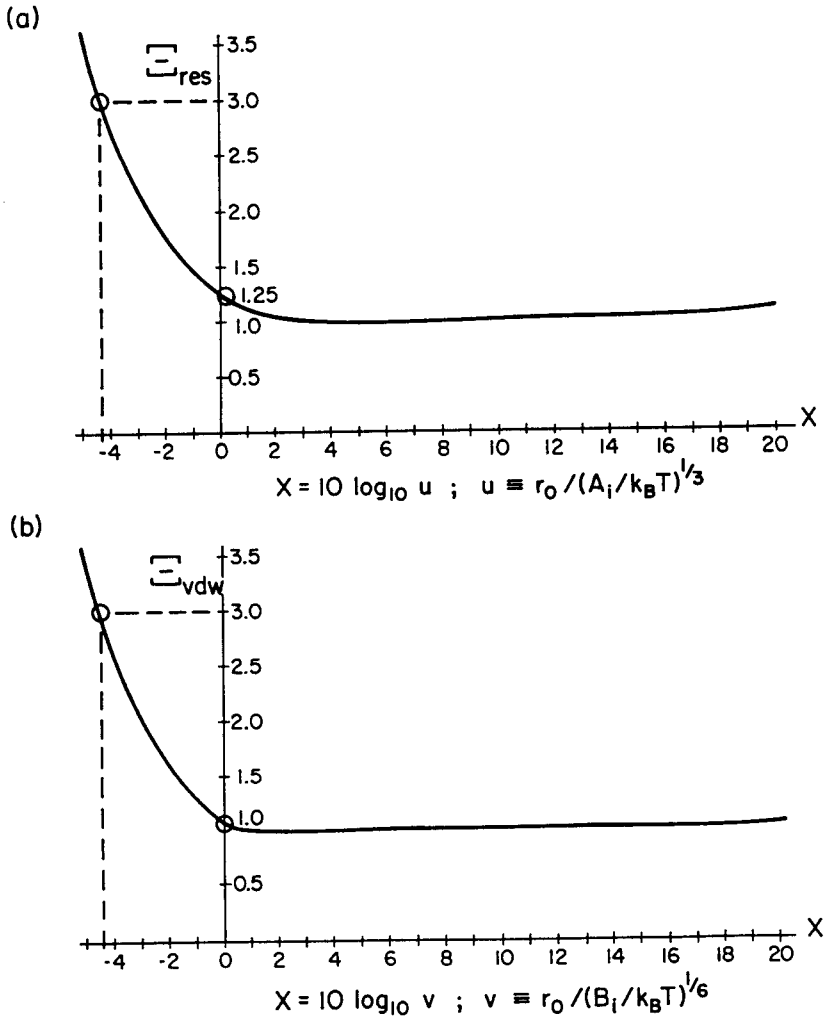

Fig. 10. A graph of (a) Ξ_{res} as a function of $x = 10 \log_{10} u$, where $u \equiv r_0/(A_i/k_BT)^{1/3}$ and (b) Ξ_{vdw} as a function of $x = \log_{10} v$, where $v = r_0/(B_i/k_BT)^{1/6}$.

is found from Figure 10a that u must be greater than approximately 1.25 which translates itself into the requirement that $A_i \leqslant 1.3 \times 10^{-37}$ Jm^3. Similarly, using the the data for the van der Waals interaction plotted in Figure 10b, it is found that in order for this interaction to yield $\Xi \cong 3.0$, it is required that $v \equiv r_0/(B_i/k_BT)^{1/6}$ be less than 0.4 which means that $B_i \geqslant 4 \times 10^{-51}$ Jm^6. On the other hand, for the van der Waals interaction to be negligible in this process, it is clear from Figure 10b, that v must be greater than 1.0 which means that $B_i \leqslant 1.7 \times 10^{-53}$ Jm^6.

Based on these results, a number of interesting conclusions can be inferred. First of all, assuming that the resonant long-range interaction is entirely responsible for the process of accelerated rouleau formation, this can only be possible in a non-equilibrium situation with $f_- \cong 0.0$ and $f_+ \cong 1.0$ (occupation inversion). Assuming after Fröhlich (1980) that $\omega \sim 10^{11}$ Hz, it is fully justified to adopt the classical limit in the calculations. Therefore, with these assumptions from Equation (23) and (24), the condition is obtained that $A_c^2/B_c = 2nk_BT \geqslant 10^{-18}$ J. This gives the lower limit on the number of quasiparticles occupying the selected dipole mode (ω_+) as

$n \geqslant 120$. If the other case is to be realized, i.e. that under occupation inversion conditions the van der Waals attraction is to be predominantly responsible for the rouleau formation, then the corresponding condition is $n \leqslant 10^{-3}$ (i.e. no dipole modes may be excited in the system) and, thus, can be excluded as a viable option. However, in the thermodynamic equilibrium case, by and large, the long-range interaction can be excluded as a possible cause of rouleau formation, as discussed earlier. The feasibility of the process being carried out through the van der Waals attraction will be discussed later. In order to be able to estimate the frequencies involved in the process some important parameters must be evaluated. In agreement with the experimental conditions, the dipole separation r is chosen to be twice the diameter of an erythrocyte, i.e. $r = 16$ μm. The mass M is that of each of the Z elastically bound particles, protons, i.e. $M = 1.67 \times 10^{-27}$ kg. With the configuration of Figure 3, substituting the relevant data, i.e. the distance between the effective dipolar layers $r \approx 10$ μm and $\gamma_0 \approx 20°$, into the formula for γ given below Equation (5) it is found that $\gamma \approx 0.1$. The three main polypeptides of an erythrocyte ghost are known as spectrin, tektin A and myosin and their combined number reaches approximately $N \cong 1.5 \times 10^6$ per ghost (De Robertis and De Robertis, 1980). Using $n \cong 200$ for the number of dimers per polypeptide (Rabinowitz, 1984) and also for the occupation number of the dipole mode, their product is obtained as $Z = Nn \cong 3 \times 10^8$. This when used in Equation (23) requires the resonant frequency of $\omega = 2 \times 10^{12}$ Hz (or less) in order for $\Xi_{res} \cong 3.0$. This is somewhat high on the frequency range predicted by Fröhlich but nonetheless within the general ballpark. It must be emphasized here that several of the numbers used for this calculation are only rough estimates than exact figures. Had we used $Z = 5 \times 10^7$ (meaning, for example, that not all the polypeptides participated in the interaction but only a small fraction, due, say, to the geometry of the erythrocyte), then the resonant frequency producing $\Xi_{res} = 3.0$ would be approximately 3×10^{11} Hz, at the lower end of the range predicted by Fröhlich. For ω greater than 10^{13} Hz, the corresponding Ξ_{res} tends to its random motion value.

For coagulation to result entirely from the van der Waals interactions we use Equation (24) and the number $B_i = 4 \times 10^{-51}$ Jm^6 as read off Figure 9b and find that, with the value of $Z = 3 \times 10^8$, any frequency in the range lower than 10^{11} Hz is capable of causing a rouleau formation at the measured rate of $\Xi = 3.0$ and under conditions of thermodynamic equilibrium. For frequencies above 10^{12} Hz, the van der Waals interaction cannot increase Ξ_{vdw} above its Brownian motion value. These values of ω calculated for the van der Waals interaction are relatively insensitive to a variation of Z since as seen from Equation (24) $\omega \sim Z^{1/2}$. Thus, in terms of the required frequency range, this result is less uncertain than that obtained for the long-range interaction.

Finally, we comment on the use of free water parameters for the dielectric properties of the medium. In the range of interest to us the sign of $\partial\varepsilon'/\partial\omega$ is negative for practically all biological substances of importance to this study (Grant *et al.*, 1978), i.e.s for water, aqueous solutions of hemoglobin, blood, solutions of myoglobin, etc.

Taking into account the concentration of NaCl (c = 150 mM) used in the relevant experiments results in a negligible decrease of the relaxation time τ by approximately 1.5% and of the static dielectric constant ε'_s by approximately 4%. This would have a very minor modifying on our calculations. The electric fields of the order of magnitude present in the membrane do not drastically affect the dielectric properties of the constituent water (Hasted, 1973). Lastly, raising the temperature close to the upper physiological limit of 40°C results in ε'_∞ dropping very little below its value at 20°C, ε'_∞ dropping by about 10% while the relaxation time decreases by almost 50%. From Equation (11) and (12), then follows that the range of frequencies leading to strong long-range forces should be shifted upwards rather significantly with the increase of temperature.

5. Discussion and Conclusions

In the past, there were a number of theoretical models put forward in an effort to explain rouleau formation. Ponder (1957) suggested that the macromolecules are adsorbed on the cell's surface and, as a result, alter the local dielectric constant of the membrane. This could cause an expansion of the double layer and an increase of the surface potential. However, to achieve sufficiently strong attraction between erythrocytes, the dielectric constant would have to reach unrealistically high values. Ross and Ebert (1959) proposed that dextran causes a rearrangement of surface proteins which leads to an increase in the surface charge density. Sieh and Sterling (1969) pointed out to a nonspecific anion binding to an adsorbed polymer layer as a possible reason for an increase in the surface charge. Brooks (1973) and Brooks and Seaman (1973) advanced a model which shows an increase of the zeta potential as a result of polymer adsorption and an associated expansion of the double layer, provided the concentration of dextran exceeds a threshold value. The red cell aggregation is then envisaged as resulting from nonspecific cross-linking of polymer between adjacent cell surfaces. This mechanism could occur only if the polymer's molecular weight was large enough to allow for sufficiently long bridges. However, there appears to be no concrete evidence in support of the cross-linking hypothesis. Recently, Evans (1986) suggested another possible mechanism, i.e. depletion flocculation which is a process where free polymer is squeezed out in the small gap between the two interacting red blood cells. This would then yield an attractive force at small distances which is due to an osmotic pressure between the gap and the solution. However, this mechanism could not explain the observations of Rowlands *et al.* (1981, 1982) which indicate that erythrocytes attract each other over long ranges on the order of 10 μm. All the other mechanisms discussed here could not account for some important features of rouleau formation revealed by experiment, e.g. sensitivity to the pH-level, species recognition or dependence on metabolic activity.

Metabolic activity is associated with a sufficient supply of ATP. A drop of ATP to 1/2 of its normal value leads to abrupt crenation and sphering of the cells. It does

not, however, change the zeta potential or the surface charge (Weed *et al.*, 1969). The transmembrane potential can be reduced either by a drop in the pH from its normal value of 7.6 or by treating the cells with ionophore. Both of these effects cause sphering since the lowering of the pH is associated with a reduction of surface charge, that would lead to less repulsion between cells and higher rate of aggregation which could not be explained using a purely electrokinetic model. Moreover, since surface charges are neutralized by counter-ions up to very short distances of approach (~ 1 nm), the electrostatic forces are certainly short range in these solutions. Cellular organization can be destroyed by the presence of gluteraldehyde in the solution which cross-links proteins without any effect on the cell's shape, area or volume. The experiment of Sewchand and Rowlands (1983) also indicates a certain amount of specificity in the erythrocyte interactions. Namely, contrary to standard predictions for colloidal coagulation, cells from different species tend to adhere less than those from a single species. Moreover, further experiments of Rowlands *et al.* (1983) involved micro-manipulation of rouleau and were intended to investigate the nature of binding betwen erythrocytes. It was found that erythrocytes are joined by contractils, which are 10–100 μm long fibrils made of macromolecules. The conditions which are required for the formation of contractils exactly mirror those required for rouleau formation itself. However, the erythrocyte interaction takes place before cellular contact has been made while contractils arise after contact. This would indicate that macromolecules may be involved in transmitting or facilitating the interaction but are not themselves responsible for the onset of rouleau formation. Moreover, there are indications that contractils do not produce just visco-elastic forces as evidenced by an unusually rapid pulling together of the cells when a contractil breaks and by the fact that the line of attachment of a contractil to a cell is always directed radially towards the center of the cell.

The results of these observations have been rather hastily interpreted as lending significant support to the theory of Fröhlich (Paul *et al.*, 1983). The objective of this paper was to quantitatively verify whether or not this model is capable of explaining the experimental results. Our findings have led to the identification of two possible scenarios. First, under nonequilibrium conditions of externally supplied energy being pumped to occupy the higher of the two levels (ω_+), and assuming that the frequency is in the upper end of the 10^{11}–10^{12} Hz range, the resultant rate of rouleau formation does indeed reach the measured value of $\Xi = 3.0$ supporting the predictions of Fröhlich. It should also be emphasized that the resonant frequency of 0.367×10^{11} Hz detected by Blinowska *et al.* (1985) is very close to the characteristic frequency ω^* of 0.41×10^{11} Hz (see Figure 4) at which the two eigenfrequencies ω_+ and ω_- begin to split. At this point of our investigations it is not entirely clear through what physical mechanisms the occupation inversion with $f_+ \cong 0.0$ is to be realized in the membrane. Using the numbers presented in this paper it is easy to calculate the energy required for the occupation inversion to be on the order of 10^{-15} J. This is not an unreasonably high amount of

energy for a biological cell to accumulate. It may, for example, be obtained through the supply of ATP resulting via the process of hydrolysis in the creation of approximately 10^5 elementary units of energy (0.205 eV each). The energy released in the ATP-ADP transformation can be transmitted losslessly through the membrane via solitons (Davydov, 1985) which may polarize the membrane and create an electret state as pointed out by Del Giudice *et al.* (1985). Within this scenario, the drop from $\Xi = 3.0$ to $\Xi \cong 1.0$ would come about as a result of insufficient supply of energy (in the form of Davydov solitons) leading to depolarization of the membrane, a subsequent reversal of the occupation levels to their thermodynamic equilibrium values, and eventual elimination of the long-range force.

The other scenario is based entirely on van der Waals forces acting between the erythrocytes. This involves arbitrary frequencies in the range below 10^{11} Hz and requires no far-from-equilibrium effects in order that Ξ may reach a value of $\Xi \cong 3.0$. Then, the drop of Ξ from 3.0 to 1.0 could be explained following the comments of Müller-Herold *et al.* (1987). Namely, as demonstrated by several experiments (Weed *et al.*, 1969; Lutz *et al.*, 1977; Nakao *et al.*, 1960), metabolic depletion and pH-reduction effects dramatically change several important physical properties of an erythrocyte. The shape changes from a biconcave disk to a crenated sphere, to a smooth sphere. Simultaneously, the measured viscosity of depleted ghosts increases several times while membrane deformability markedly decreases together with a ten-fold increases in the negative pressure required to deform the membrane. As can be seen from Equation (1) and (2), these effects would be reflected in a substantial decrease of Ξ as measured by Rowlands *et al.* (1981, 1982) and Fritz (1984). It is our intention to examine this possibility in more detail in a near future. Ultimately, a definitive explanation of the physics of rouleau formation should cover not only the origins of the inter-erythrocyte potential but also the causes of the structural changes taking place within each erythrocyte during the process.

While the present calculations cannot conclusively point to any of the two indicated possibilties as the mechanism of rouleau formation, the resonance experiments of Blinowska *et al.* (1985) would seem easier to explain using the assumption about the onset of long-range coherence. It is also tempting to interpret the experiments involving erythrocytes of two different species, following the original idea of Fröhlich (1980), as indicative of the specificity arising from a single resonant frequency (or a narrow frequency band) characteristic of a species. Fröhlich (1978, 1980) gave general arguments on how and why a cell can construct and maintain its characteristic frequency standard. Unfortunately, no convincing experiments or detailed calculations exist to date to support these statements. A more definitive answer to this problem and to the question of what is the microscopic mechanism of rouleau formation requires further model calculations and, of course, more refined experiments. Suggestions presented by Müller-Herold *et al.* (1987) seem especially suitable as a starting point for future calculations involving rouleau formation.

There are, however, serious drawbacks inherent in the Fröhlich theory. First of all, it requires the occupation inversion of the energy levels achieved through an unspecified mechanism. Secondly, it assumes a narrow band of frequencies resulting from Bose condensation. On the other hand, the dynamic van der Waals interaction requires no difficult preconditions and it works well as long as the frequencies do not exceed certain values. It is worth noting that the van der Waals forces were considered a possible mechanism of rouleau formation before by Gingell and Parsegian (1971) but our present model invokes dynamic rather than static dipole-dipole interactions. Unfortunately, it will not be easy to explain some more intricate effects such as specificity or nonthermal behavior using the van der Waals forces alone. It is conceivable, however, that both the resonant and the van der Waals forces can be at play simultaneously, the former arising and being dominant under very special circumstances while the latter being present in all situations and dominant in most cases.

Acknowledgements

This research has been supported by a grant from the Natural Sciences and Engineering Research Council of Canada. The authors express their gratitude for technical assistance to Mr B. Ramjattan. Useful discussions with Dr K. J. Blinowska and Dr G. Vitiello are gratefully acknowledged.

References

Blinowska, K. J., Lech, W., and Wittlin, A. (1985) *Phys. Lett. A* **109**, 124.
Brooks, D. E. (1973) *J. Coll. Interface Sci.* **43**, 687; 707; 714.
Brooks, D. E. and Seaman, G. V. F. (1973) *J. Coll. Interface Sci.* **43**, 670.
Chance, B., Mueller, P., De Vault, D., and Power, L. (1980) *Physics Today* **80**, 32.
Davydov, A. S. (1985) *Solitons in Molecular Systems*, D. Reidel, Dordrecht.
Del Giudice, E., Doglia, S., Milani, M., and Vitiello, G. (1985), *Nucl. Phys. B* **251**, 375.
De Robertis, E. D. P. and De Robertis, E. M. F. Jr. (1980) *Cell and Molecular Biology*, Holt, Rinehart and Winston, New York.
Evans, E. (1986) *Biorheology* **23**, 192.
Fritz, O. G. (1984) *Biophys. J.* **46**, 219.
Fröhlich, H. (1958) *Theory of Dielectrics*, Oxford University Press, London.
Fröhlich, H. (1972) *Phys. Lett. A* **39**, 153.
Fröhlich, H. (1978) *IEEE Trans., MIT* **26**, 613.
Fröhlich, H. (1980) *Adv. Electron. Electron. Phys.* **53**, 85.
Gingell, D. and Parsegian, V. A. (1971) *Biophys. Soc. Abstracts*, 15th Annual Meeting.
Grant, E. H., Sheppard, R. J., and South, G. P. (1978) *Dielectric Behavior of Biological Molecules in Solution*, Oxford University Press, Oxford.
Hasted, J. B. (1973) *Aqueous Dielectrics*, Chapman and Hall, London.
Lutz, H. U., Liu, S. C., and Palek, J. (1977) *J. Cell. Biol.* **73**, 548.
Müller-Herold, U., Lutz, H. U., and Kedem, O. (1987) *J. Theor. Biol.* **126**, 251.
Nakao, M., Nakao, T., and Yamazoe, S. (1960) *Nature* **187**, 945.
Paul, R., Chatterjee, R., Tuszyński, J. A., and Fritz, O. G. (1983) *J. Theor. Biol.* **104**, 169.
Pokorny, J. (1980) *Czech. J. Phys. B* **30**, 1339.
Ponder, E. (1957) *Révue d'Hématologie* **12**, 11.

Reich, R. R. (1978) *Hematology: Physiopathologic Basis for Clinical Practice*, Little, Brown, New York.
Ross, S. W. and Ebert, R. V. (1959) *J. Clin. Invest.* **38**, 155.
Rowlands, S., Sewchand, L. S., Lovlin, R. E., Beck, J. S., and Enns, E. G. (1981) *Phys. Lett. A* **82**, 436.
Rowlands, S., Sewchand, L. S., and Enns, E. G. (1982) *Phys. Lett. A* **87**, 256; *Can. J. Physiol. Pharm.* **60**, 52 (1982).
Rowlands, S., Eisenberg, C. P., and Sewchand, L. S. (1983) *J. Biol. Phys.* **11**, 1.
Sewchand, L. S. and Rowlands, S. (1983) *Phys. Lett. A* **93**, 363.
Sieh, J. B. and Sterling, C. (1969) *Biochim. Biophys. Acta* **184**, 281.
Steck, T. L. (1974) *J. Cell. Biol.* **62**, 1.
Tuszyński, J. A. (1985) *Phys. Lett. A* **107**, 228.
Webb, S. J. (1980) *Phys. Rep.* **4**, 201.
Weed, R. I., La Celle, P. L., and Merrill, E. W. (1969) *J. Clin. Invest.* **48**, 795.